

**Right Ventricle Curvature Maybe a Predictor for Pulmonary Valve
Replacement Surgery Outcome: A Multi-Patient Study**

A Project Report

Submitted to the Faculty of

WORCESTER POLYTECHNIC INSTITUTE

in Partial Fulfillment of the Requirements of the

Degree of Doctor of Philosophy

by

Heng Zuo

Date: August 27, 2014

Approved by,

Professor: Dalin Tang, Advisor

Professor: Tal Geva, MD, Co-Advisor

ABSTRACT

Patients with repaired tetralogy of Fallot (TOF) account for the majority of cases with late onset right ventricle (RV) failure. The current surgical approach, which includes pulmonary valve replacement/insertion (PVR), has yielded mixed results in terms of RV functional recovery. Therefore, it is of great interest for clinicians to identify parameters, which may be used to predict post-PVR outcome.

Pre- and post-PVR cardiac magnetic resonance (CMR) data were obtained from 60 repaired TOF patients with consent obtained for analysis. RV ejection fraction (RVEF) change (post-PVR RVEF minus pre-PVR RVEF) was used to measure post-PVR improvement. The patients were divided into Group 1 (optimal outcome) and Group 2 (poor outcome) for comparison. RV wall thickness (WT) and curvature were obtained from CMR data for statistical analysis.

Using mean quarter values (one CMR slice = 4 quarters), statistically significant differences in circumferential curvature (C-curvature) and longitudinal curvature (L-curvature) at end-diastole (maximum RV volume) and WT and C-curvature at end-systole (minimum RV volume) between Group 1 and Group 2 were found.

Correlations between average WT at systole and between L-curvature at diastole and the change of RVEF were statistically significant. Specifically, the correlation coefficient between average WT at systole and change of RVEF was -0.2715 , ($p = 0.036$) and between L-curvature at diastole and change of RVEF 0.3297 ($p = 0.01$). This initial study suggests that the RV longitudinal curvature and wall thickness may be used as a marker/predictor for PVR surgical outcome.

ACKNOWLEDGEMENT

I would like to express my deepest gratitude to Professor Dalin Tang, my advisor, for his tremendous help, constant encouragement, patient guidance, and thoughtful advice during my project and my study at Worcester Polytechnic Institute. Without his help and support, this project would never have been completed. I would also like to sincerely thank Professor Tal Geva (Children's Hospital, Boston, Harvard Medical School), co-advisor of my project, for his valuable guidance, help and encouragement and providing me the opportunity to do the curvature work in the Department of Cardiology at Children's hospital Boston. His numerous suggestions and support have made my project possible. Finally, I would also like to thank my parents for their constant love and emotional support during my studies here.

Acknowledgement: NIH-1R01-HL 089269 (del Nido, Tang, Geva), NIH-HL63095 (PI: del Nido) and NIH-NHLBI 5P50HL074734 (PI: Geva; Co-Investigator: del Nido).

TABLES OF CONTENTS

ABSTRACT.....	2
ACKNOWLEDGEMENT.....	3
TABLES OF CONTENTS.....	4
LIST OF FIGURES	6
LIST OF TABLES.....	6
1. INTRODUCTION AND BACKGROUND.....	7
1.1 Introduction.....	7
1.2 Description of the Clinical Problem.....	8
1.3 Mechanism of RV Dysfunction in Repaired ToF patients.....	9
1.4 Current Management of Failing RV in ToF Patients.....	10
2. METHODS.....	12
2.1 CMRI data acquisition	12
2.2 RV Volume and RVEF	14
2.3 Processing of original data	18
2.4 Geometrical Analysis	19
3. RESULTS AND ANALYSIS.....	23

3.1 Correlation Results.....	23
3.2 Comparison Results.....	25
4. DISSCUSSION.....	27
5. CONCLUSIONS.....	29
REFERENCES.....	30

LIST OF FIGURES

Figure 1. Repaired Tetralogy of Fallot (ToF) heart with RV outflow patch and scar.....	10
Figure 2. Basic plots showing curvature analysis using data from a healthy volunteer.....	13
Figure 3. Shows pre-operative CMR images and segmented MRI contour plots from a patient with repaired TOF.....	14
Figure 4. 3D stacked segmented RV/LV of one patient before PVR at end of systole and end of diastole.....	15
Figure 5. RV inner contour with series of triangles.....	16
Table 1. Results of RVEF, change of RVEF and classification.....	18
Table 2. Comparison results of two groups on WT/C-curvature/L-curvature.....	24
Table 3. Correlation results between WT/C-curvature/L-curvature and Change of RVEF.....	26

1. Introduction and background

1.1 Introduction

Patients with repaired tetralogy of Fallot (ToF), a congenital heart defect comprised of ventricular septal defect and severe right ventricular outflow obstruction, account for the majority of cases with late onset RV failure. The current surgical approach, which includes pulmonary valve replacement (PVR), has yielded mixed results with many patients not recovering RV function after PVR with or without concomitant RV remodeling surgery [1]. For patients with ToF who need PVR surgery, surgical intervention such as scar tissue resection and anterior wall RV remodeling have been proposed in order to improve RV function recovery [2]. While our patient-specific models supported the RV remodeling approach [3], data from our clinical trial showed only modest improvement in RV ejection fraction ($-2\pm 7\%$ in the PVR-alone group (n=34) vs. $-1\pm 7\%$ in the PVR with RV remodeling group (n=30); $P=0.38$) at 6-month postoperative follow-up [4].

Indicators that can be used to identify patients with better outcome after PVR are urgently needed. It is clear that the RV morphology must have some close relationship with RV function. Maybe we can find the indicators from RV morphology.

The objectives of this Project are:

1) Conduct some morphological study (e.g., wall curvature) on 60 patients randomly selected from our clinical trial data pool (with IRB approval and consent obtained).

2) To perform statistical analysis on the results of the morphological study for searching for the indicators that can identify patients with better outcome after PVR.

This project provided an opportunity for the author to learn directly from cardiologists, cardiac radiologist, and other medical professionals at Boston Children's Hospital, Harvard

Medical School. This is a great help for the author to better understand the biological background of heart circulation.

1.2 Description of the Clinical Problem

Tetralogy of Fallot (ToF) is a congenital heart malformation that comprises a ventricular septal defect, rightward malposition of the aorta, infundibular pulmonary stenosis, and right ventricular hypertrophy. The malformation is thought to result from underdevelopment of the subpulmonary infundibulum during early embryonic development with all elements of the anomaly resulting from this abnormality. ToF is the most common cyanotic cardiac defect, with an incidence of 3.26 per 10,000 live births, or about 1300 new cases per year in the United States [5].

The anomaly begins during early embryonic development with a narrowed pulmonary valve and a defect between the ventricles (called ventricular septal defect or VSD). The defect is tolerated well by the fetus because only a small amount of blood flows through the lungs until birth. After birth, the blood that is supposed to start flowing through the lungs cannot easily get there due to the narrowed right ventricular outflow tract and pulmonary valve; however, the ventricular septal defect remains open so that much of the blood that comes back to the heart needing oxygen is sent out without being properly oxygenated. In addition, the right ventricle (RV) has to pump at the same pressure as the left ventricle (LV). Several changes follow. First, the baby turns cyanotic because the deoxygenated blood that bypasses the lungs mixes with the oxygenated blood and lowers the oxygen saturation of the systemic blood. Deoxygenated blood is darker and appears blue through the skin. Second, the right ventricle hypertrophies from the increased pressure load imposed on it. Next, the low oxygen saturation of the systemic blood causes it to get thicker (i.e., higher concentration of red blood cells) and clot more easily. Clots

in the veins can now pass through the ventricular septal defect and directly enter the aorta, where they can do much more damage than in the lungs—such as causing infarcts in the brain [6].

Since surgical repair of ToF was first performed over 45 years ago, survival of these patients has greatly improved with recent reports showing a 20-year survival rate nearing 90% [7, 8]. However, in long-term follow-up, considerable and rising late morbidity and mortality are encountered, which is related to right ventricular (RV) dysfunction/dilatation and heart failure.

1.3 Mechanism of RV Dysfunction in Repaired ToF patients

After surgical repair of ToF, most patients have an excellent functional result and lead a normal active and social life. Nevertheless, surgical repair of ToF usually comprises incision into the right ventricular outflow tract (RVOT), removal of obstructive cardiac muscle, removal of obstructive pulmonary valve tissue, and placement of a patch made of non-contracting tissue or synthetic material to widen the RVOT and pulmonary valve annulus. Consequently, the majority of these patients have residual hemodynamic abnormalities, primarily due to chronic pulmonary regurgitation (PR) that leads to RV volume overload. Additional hemodynamic abnormalities such as residual RVOT obstruction, branch pulmonary artery stenosis, tricuspid regurgitation, or a residual ventricular septal defect can further aggravate right and/or left ventricular dysfunction [9]. Thus, although early results with surgical repair of ToF are very good, late results are not as good and many if not most of these patients develop progressive right ventricular dilatation and dysfunction over time. Paradoxically, due to the improved survival with surgery for ToF in infancy achieved in the 80s, the number of ToF patients presenting in their third and fourth decade of life with severe RV dilation and dysfunction is growing rapidly.

1.4 Current Management of Failing RV in ToF Patients

The surgical treatment of patient with repaired ToF presenting with RV dysfunction traditionally has been to eliminate the defects that directly impact on RV volume with the thought that RV dilatation per se, contributes to RV dysfunction. Thus, much of the emphasis has centered on elimination of pulmonary regurgitation by replacing/inserting a prosthetic pulmonary valve, and reduction of the RV outflow patch (Fig. 1 (b)).

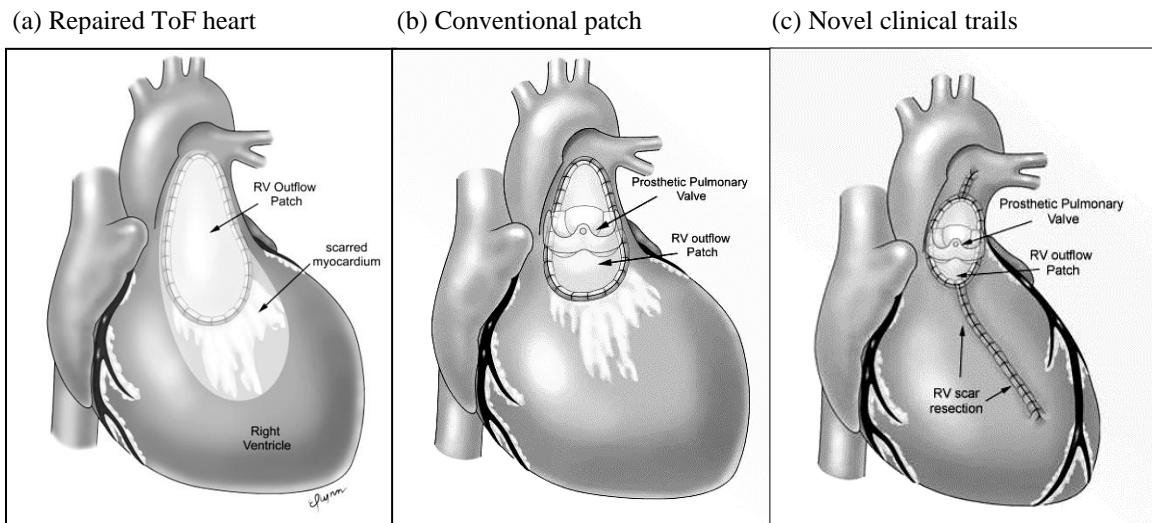


Figure. 1. Repaired Tetralogy of Fallot (ToF) heart with RV outflow patch and scar [2]. (a) ToF heart with RV outflow patch and scar on anterior RV wall, large shaded area indicates area of akinesis/dyskinesis; (b) Current management: Heart after pulmonary valve insertion (PVR) and reduction of RV outflow patch; (c) Novel clinical trial (surgical RV remodeling): PVR, reduction of RV outflow patch and removal of RV scar.

Studies evaluating the results of this approach indicate that in most patients there is a significant decrease in RV end-diastolic volume [10], which is the index used to assess volume load of the ventricle. However more recent studies focusing on RV function after surgery have found mixed

results. Some clinical reports indicate that the surgical treatments result in decrease in RV volume and some improvement in RV function, while in others showing no significant improvement in RV function after surgery. The differences in these findings may relate to methodology such as use of magnetic resonance imaging (MRI) in the latter studies, but likely also indicate that there is significant heterogeneity in this patient population. There are some reports indicating that the worse systolic function pre-operatively in the latter group may have contributed to the lack of improvement in RV function with pulmonary valve replacement/insertion (PVR) alone. The lack of predictable improvement in ejection fraction after PVR alone is of concern, and suggests that persistent RV dysfunction is a marker of adverse remodeling with scar formation and fibrosis, and that conventional procedures with PVR alone are not enough for many patients.

2. METHODS

2.1 CMRI data acquisition

Cardiovascular magnetic resonance (CMR) is established in clinical practice for the diagnosis and management of congenital and acquired heart diseases [5, 12]. In contrast to 2-D echocardiography, angiocardiology, and radionuclide techniques, CMR does not rely on geometrical assumptions, is accurate regardless of the shape or orientation of the chamber, and most investigators now consider it the gold standard imaging modality for assessment of ventricular dimensions and function [13,14,15, 16]. Noninvasive CMR techniques have enabled to quantify the geometry, blood flow in any desired location, including quantification of pulmonary regurgitation and measure biventricular systolic function [17, 18].

CMR data before and six months after PVR surgery were obtained from 60 patients (40 male, 20 female) with consent obtained for analysis. A recent detailed review of CMR imaging techniques for congenital heart disease was given by Brown, Powell and Geva [19]. For our study, cardiac MRI (CMR) studies were performed in a dedicated MRI suite located in the Department of Cardiology at Boston Children's Hospital to acquire patient-specific ventricular morphology, flow velocity, and flow rate for patients needing pulmonary valve replacement operations before and after scheduled surgeries and healthy volunteers. Using ECG-gated steady state free precession cine MRI, 12–14 contiguous slices were obtained in the ventricle short-axis plane covering the left and right ventricles from the plane of the AV valves through the apex. In each location, 30 phases were acquired during one cardiac cycle. For the purpose of this analysis, we used image data at end-diastole (maximal volume) and end-systole (minimal volume). Figure 2 depicts a sketch of a healthy human heart with RV, LV, a stack of RV contours, and the reconstructed RV/LV geometry obtained from a healthy volunteer.

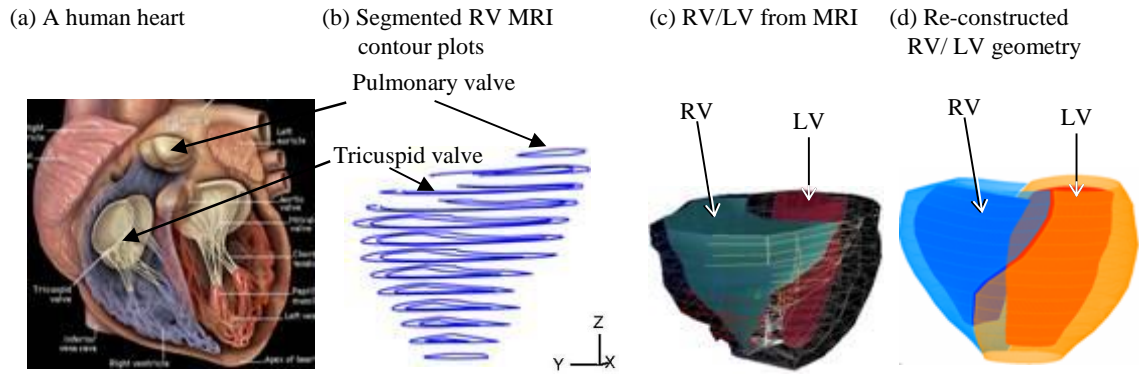
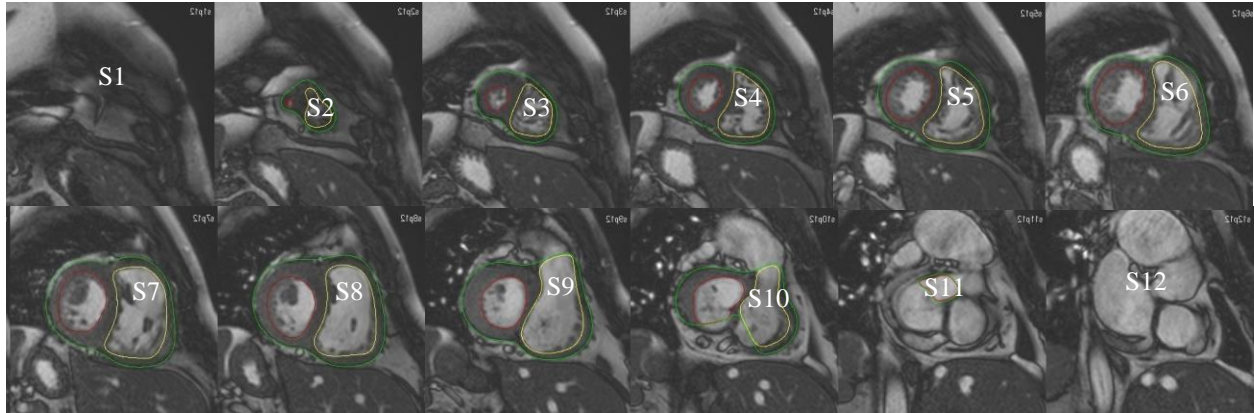


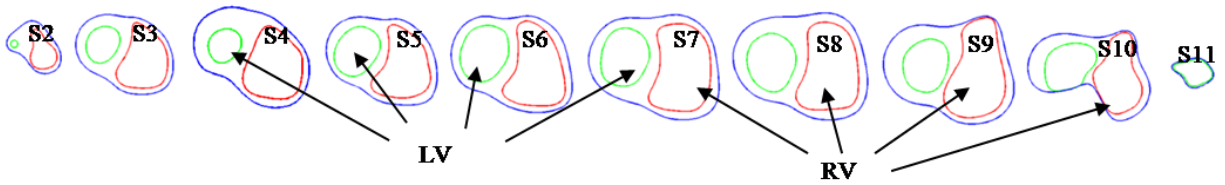
Figure 2 Basic plots showing curvature analysis using data from a healthy volunteer. (a) A human heart sketch showing left and right ventricles with valve positions; (b) segmented RV MRI contour plots; (c) RV/LV geometry from MRI; (d) the re-constructed 3D geometry of the RV/LV combination model.

Figure 3 shows pre-operative CMR images and segmented MRI contour plots from a patient with repaired TOF.

(a)



(b)



(c)

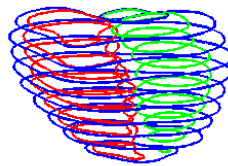


Figure 3 (a) Pre-operation CMR images (end-systole) acquired from a ToF patient and (b) segmented RV/LV contours. (c) 3D re-constructed RV/LV model.

Curvature Analysis

The morphology and function of the Right Ventricle are likely interrelated, thereby affecting the results of PVR. Therefore, we hypothesized that there may be a link between morphology of Right Ventricle and PVR outcomes. We expect that analysis of shape of the Right Ventricle identify indicators to identify patients with better functional recovery of the Right Ventricle after PVR. In this project, we focus on the curvature and wall thickness of Right Ventricle.

We are provided with 60 sets of patient-specific data, and each patient data set contains pre-operative and follow-up post-operative CMRI of this patient acquired by methods described previously. Only the CMRI of end-diastolic (volume is maximal) and end-systolic (volume is minimal) will be used in the curvature analysis.

2.2 RV Volume and RVEF

We are searching for potential indicators to identify patients with better outcome after PVR, so firstly we need to divide the 60 patients into two groups. The division is based on the change of Ejection Fraction of Right Ventricle (RVEF) from pre-operation to post-operation. For each patient data set, we have pre-operative and post-operative CMR scan at end-diastole and end-systolic, so RV Volume at end-diastole and end-systolic of before/after PVR can be measured. Then RVEF defined as $RVEF=(RVEDV-RVESV)/RVEDV$.

2.2.1 Calculate RV Volume and RVEF

For each patient data set, segmented RV/LV contours (shown in Figure 2) contain all geometrical information of RV/LV, 3D stacked contours at end-diastole and end-systolic of one patient before PVR are shown in Figure 4.

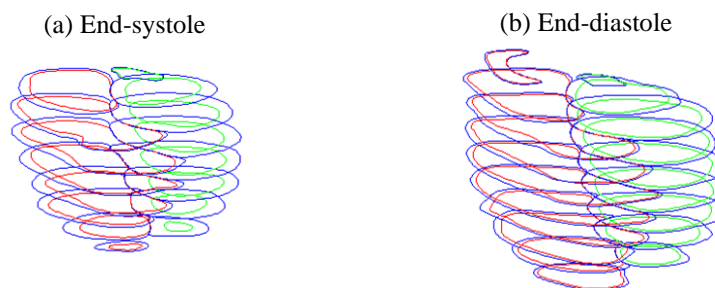


Figure 4 3D stacked segmented RV/LV of one patient before PVR at end of systole and end of diastole.

Approximating the volume of RV as the following equation,

$$RV\ Volume = \sum_{i=1}^{n-1} S_i \times d_i$$

Here, n is the number of RV inner contours, S_i is the area of i^{th} RV inner contour, d_i is the distance between two neighboring contours (between i^{th} and $(i + 1)^{th}$ RV inner contours). Since distance between two neighboring contours is a constant in one patient data set, we can use d to express the distance replacing of d_i , the RV volume is followed as

$$RV\ Volume = \sum_{i=1}^{n-1} S_i \times d$$

To measure area of each RV inner contour, at first we find the central point of the RV inner contour, then the central point will form a series of triangles with any two neighboring points on the RV inner contour (RV inner contour with series of triangles shown in Figure 5), then we can use the sum of area of these triangles to approximate the area of the RV inner contour.

So far, we obtained RV volume at end-systolic(RVESV) and end-diastolic(RVEDV), then RVEF can be calculate by $RVEF=(RVEDV-RVESV)/RVEDV$.

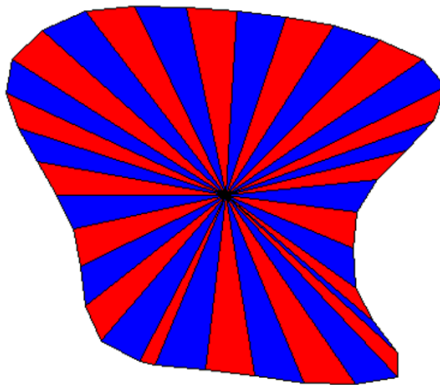


Figure 5. RV inner contour with series of triangles.

2.2.2 Classification based on RVEF

Using the method mentioned in 2.2.1, we can get RVEF of each patient before and after PVR based on CMRIs of the patient. Then we can determine the change of RVEF comparing pre-operative and post-operative results ($\text{Change of RVEF} = \text{Pre-RVEF} - \text{Post-RVEF}$). The change of RVEF will be used as the index to divide the 60 groups of patients.

We divide the 60 patients into two groups based on change in RVEF from pre-PVR to post-PVR CMR examinations. Group 1 comprised of 30 patients with the best response of RVEF to PVR (patients either had an improved RVEF or remained stable) whereas Group 2 comprised of 30 patients with the worst response (decreased RVEF after PVR). Data regarding change in RVEF and group classification are shown in Table 1.

Group 1: RVEF Increased		Group 2: RVEF decreased	
Patient ID	Change in RVEF(%)	Patient ID	Change in RVEF(%)
40	-1.63 %	31	-13.46 %
5	-1.58 %	3	-13.22 %
14	-1.28 %	26	-13 %
60	-1.11 %	20	-12.39 %
35	-1.05 %	28	-11.16 %
27	-0.64 %	21	-10.75 %
56	-0.57 %	59	-9.99 %
24	-0.4 %	41	-9.77 %
13	-0.35 %	32	-8.84 %
36	-0.18 %	25	-8.59 %
43	-0.08 %	34	-8.56 %
46	0.24 %	55	-7.61 %
4	0.95 %	54	-7.56 %
48	1.44 %	18	-7.3 %
37	1.47 %	58	-7.21 %
10	1.59 %	38	-7.18 %
33	1.73 %	29	-6.44 %
8	1.81 %	39	-6.29 %
2	1.82 %	11	-6.27 %
6	1.82 %	44	-5.75 %
51	1.86 %	22	-4.79 %
1	2.09 %	49	-4.19 %
53	2.36 %	47	-4 %
19	2.39 %	9	-3.96 %
50	2.61 %	30	-3.9 %
15	6.56 %	17	-3.75 %
12	6.59 %	45	-3.28 %
52	7.86 %	23	-3.17 %
16	8.56 %	57	-2.54 %
42	11.5 %	7	-2.07 %
mean \pm SD	1.87% \pm 3.24%		-7.23% \pm 3.36%

Table 1. Results of RVEF, change of RVEF and classification.

2.3 Processing of original data

Original data provided to us contain CMR data of pre-operation and post-operation. For each CMR data set, generally there are 11-14 slices for end-diastolic set, and 9-12 slices for end-systolic set. Slices are in the short-axis cross plane of the ventricles. In each slice, 10 different contours of the ventricles are provided in systole and diastole (e.g., RV and LV endocardium and epicardium). In the analysis described here, only inner/outer contours of Right Ventricle and Left Ventricle were utilized.

Unification and Points Matching

In the original data, we are provided with the total amount of points on each contour, and the coordinates of each point on this contour. Generally, different contours have different amount of points. For convenience in the future work, here we should unify the amount of points on each contour. Unify the amount of points on each contour to 100 equidistantly by using interpolation.

(1) Start Points Choosing:

For RV inner and outer contour in each slice, we find two corresponding points on each contour and set them as start points of the two contours. Adjust the start points of each contours to make them lay in a smooth longitudinal curve (we call it longitudinal consistency). Then starting at these points we will divide each contour into 100 segments equidistantly.

(2) Four-Special-Points Method:

Because of the similarity between inner and outer contour of Right Ventricle at the same slice, after choosing start points and equidistant division (Step (1)), points with the same number on inner and outer contours should be corresponding points. But for further work, we also need to align the points of each slice in longitude. Here we adopt **4-special-point**

method, and we will introduce this method briefly as following. Take RV inner contours as an example.

1. The four points should locate on the inner contour as equidistant as possible, which will divide the contour to 4 parts equidistantly.
2. The character of the four points should be so clear that we can find easily such points on different slices.

After finding the 4 special points on each slice, a 3D contour figure should be plotted, and then these four points will be adjusted according to the smoothness in longitude. When the adjustment is done, use the four points to re-divide the contours.

Now the four special points divide the contour into 4 parts. For each part, we divide it to 25 segments equidistantly, and then we will get a new 100 points. Now, for the points in different slice, if the points have the same number, then they will be corresponding points in the longitudinal direction. When searching for the special points, it should be done on RV inner contour and outer contour simultaneously, because we will calculate the wall thickness, so the correspondence between inner and outer contour should be also considered.

2.4 Geometrical Analysis

2.4.1 Wall Thickness

After choosing the start point and equidistant division, the points with the same number on inner and outer contours will be corresponding points, so use the coordinates in x-,y-direction of the two corresponding points can get the distance of the two points which can be considered as the thickness of the wall at the pair wise points.

2.4.2 Circumferential Curvature

Curvature is the representation of geometrical properties in mathematics. In our problem, we are considering the geometrical characteristics of the hearts, so it is a 3D problem. We will use circumferential curvature and longitudinal curvature to describe the geometry of the RV. In this part, the method to calculate circumferential curvature is introduced, and for longitudinal curvature, the method will be introduced in the next sub part.

In each slice, every point has the same coordinate in z-direction. So we can consider right ventricular inner/outer contour as a planar curve. Then the circumferential curvature at each point on an RV inner/outer contour can be calculated using:

$$\kappa_c = \frac{x' y'' - x'' y'}{(x'^2 + y'^2)^{3/2}} \quad (1)$$

where the contour was a planar curve, x,y are treated as the function of arc, and the derivatives were evaluated using neighboring points on the contour. Use Finite Difference Method to get the derivate in the formula by using discrete points. Use central difference to get a higher approximation.

For first derivate, $x'_i = \frac{x_{i+1} - x_{i-1}}{2\Delta x}$

For second derivate, $x''_i = \frac{x_{i+1} - 2x_i + x_{i-1}}{\Delta x^2}$

2.4.3 Longitudinal Curvature

As we have done, for the points in different slices, if the points have the same number, then they will be corresponding points in the longitudinal direction. Thus in 3D view, we can use a 3D curve to connect the points with same number in different slices, use $\mathbf{X}=(x(t), y(t), z(t))$ to describe this 3D curve, then we can calculate the longitudinal curvature.

L-curvature at each point on an RV inner contour can be calculated using:

$$\kappa = \frac{\sqrt{(z''(t)y'(t) - y''(t)z'(t))^2 + (x''(t)z'(t) - z''(t)x'(t))^2 + (y''(t)x'(t) - x''(t)y'(t))^2}}{(x'^2(t) + y'^2(t) + z'^2(t))^{3/2}} \quad (2)$$

where the longitudinal curve is given by $\mathbf{X}=(x(t), y(t), z(t))$, the derivatives were evaluated using points from neighboring slices vertically below and above the point being considered. Interpolations were used to obtain vertical neighboring points from the neighboring slices. One-sided formulas were used for the top and bottom slices.

2.4.4. Statistical methods

Comparison

In previous part, we divided the 60 patients into two groups based on change of RVEF of each patient, more details can be found in Tables 1 and 2. Patients with increased RVEF after PVR are included in group 1, and Patients with decreased RVEF are included in group 2. For each patient, we use quarter value as unit – for each slice, RV contours (inner/outer RV contours) were divided into four parts as we described in Part 4, take average in each part and then there are 4 average values in each contour. This kind of average values will be used as unit for comparison analysis.

For instance, if some Patient had 10 slices, for each slice, there were one inner RV contour and one outer RV contour, and for each contour 4 quarter-average values were calculated, so for this patient, there would be 40 values for inner RV and 40 values for outer RV to be used in comparison analysis.

We used T-test as our comparison analysis tool. In end of systole and end of diastole, we compared respectively quarter values of WT/C-curvature/L-curvature between two groups. We

expect to search some significant differences in these geometrical parameters (Such as WT/C-curvature/L-curvature) between two groups. If this kind of difference exists, they could be considered as the potential candidates of the indicators we desired.

Correlation

Furthermore, we desire to search some relationship between geometry and change of RVEF, and if this kind of relationship exists in WT/C-curvature/L-curvature, they can be considered potential indicators to identify patients with better outcome after PVR.

Consider change of RVEF of each patient as one variable, and here we use patient as unit, it means that only average values will be used for each patient. We also focused on WT, C-curvature, and L-curvature. Correlation analysis was done respectively between WT, C-curvature, and L-curvature and change of RVEF at two times (end of systole and end of diastole).

3. Results and Analysis

3.1 Comparison

We use OFFICE EXCEL code ‘ttest’ to do comparison analysis here. Simple introduction about this ‘ttest’ is as following:

TTEST(array1,array2,tails,type)

Array1 is the first data set,Array2 is the second data set. In our problem, Array 1 is data of group 1, and Array 2 is data of group 2. Tails specifies the number of distribution tails. If tails = 1, TTEST uses the one-tailed distribution. If tails = 2, TTEST uses the two-tailed distribution. Here we adapted two-tailed. Type is the kind of t-Test to perform, and we use type=2 meaning Two-sample equal variance (homoscedastic).

At end of systole (volume is minimal) and end of diastole (volume is maximal), we compared two groups on WT, C-curvature and L-curvature, and the results are shown in TABLE 2.

		Vmin (end of systole)			Vmax (end of diastole)			
Data Pts		WT	C-Cur	L-Cur	Data Pts	WT	C-Cur	L-Cur
Group 1	Mean (1151Qts)	0.4017	0.8078	0.4749	Mean (1355Qts)	0.2888	0.5672	0.4253
	Stdev	0.2134	0.7361	0.2872	Stdev	0.1406	0.3774	0.2453
Group 2	Mean (1131Qts)	0.4738	0.9504	0.4613	Mean (1407Qts)	0.2994	0.6251	0.4020
	Stdev	0.2857	0.9476	0.2825	Stdev	0.1545	0.5178	0.2595
	p-value	<0.001	<0.001	0.25	p-value	0.059	<0.001	0.015

Table 2. Comparison result of two groups on WT/C-curvature/L-curvature.

P-value is less than 5% (0.05) means that difference is significant. So from the table, we can see that at end of diastole, the better outcome patients (Group 1) have larger L-curvature and lower C-curvature, and the two differences are significant. At end of systole, the better outcome

patients (Group 1) have lower wall thickness and C-curvature, and the two differences are also significant.

Thus, we can take WT and C-curvature at end of systole and C-curvature and L-curvature at end of diastole as candidates for the indicator.

3.2 Correlation

Here, we use MATLAB code 'corrcoef' to do correlation analysis, and simply introduction of 'corrcoef' is shown below.

$R = \text{corrcoef}(X)$ returns a matrix R of correlation coefficients calculated from an input matrix X whose rows are observations and whose columns are variables. The matrix $R = \text{corrcoef}(X)$ is related to the covariance matrix $C = \text{cov}(X)$ by $\text{corrcoef}(X)$ is the zeroth lag of the normalized covariance function, that is, the zeroth lag of $\text{xcov}(x, 'coeff')$ packed into a square array.

$[R,P]=\text{corrcoef}(\dots)$ also returns P , a matrix of p-values for testing the hypothesis of no correlation. Each p-value is the probability of getting a correlation as large as the observed value by random chance, when the true correlation is zero. If $P(i,j)$ is small, say less than 0.05, then the correlation $R(i,j)$ is significant.

R shows the linear correlation coefficient and P shows the significance of the correlation between the tested variables. At end of diastole and end of systole, we used 'corrcoef' to calculate the correlation between WT, C-curvature, and L-curvature and change of RVEF, and the results are shown in TABLE 3.

	Change of RVEF, end of systole(Vmin)		Change of RVEF, end of diastole(Vmax)	
	R	P	R	P
Wall Thickness	-0.2715	0.0359	-0.0988	0.453
C-curvature	-0.0964	0.464	-0.0017	0.990
L-curvature	0.2313	0.0754	0.3297	0.0101

Table 3. Correlation results between WT/C-curvature/L-curvature and Change of RVEF

From the results, P-value shows that only WT at end of systole and L-curvature at end of diastole have significant correlation with Change of RVEF. For other variants, P-value was greater than 5% showing that correlation is not significant.

In Part 3.1, results of comparison between two groups indicated that WT/C-curvature at end of systole and C-curvature/L-curvature at end of diastole may be taken as the candidates for the indicator. Combining the results of correlation analysis, we only focused on WT at end of systole and L-curvature at end of diastole now.

For WT at end of systole, R is -0.2715. For L-curvature at end of diastole, R is 0.3297. The two R values show that linear relationship between WT/L-curvature and Change of RVEF is not strong.

4. Discussion

Motivation to use computational models and shape analysis to identify potential risk predictors.

To our knowledge, the analysis of RV geometry as a potential predictor for post-PVR cardiac function outcome presented in this work has not been previously done. Nowadays, since the number of late survivors of tetralogy of Fallot repair increases rapidly, surgical management of patients with right ventricular dysfunction has become a major clinical challenge. The wide variability in clinical status, RV morphological variations, regurgitation at both tricuspid and pulmonary valves, extent of right ventricular dilatation, scarring, and dysfunction at the time of presentation has resulted in disparate surgical results with pulmonary valve insertion. The current study is adding morphological analysis as a new investigating tool and curvature/wall thickness as new potential predictors for post-operative outcome after PVR. The results of this study have yielded encouraging results: WT at end of systole and L-curvature at end of diastole stands out as the best predictor among the 6 parameters examined. In this study we analyzed CMR data from 60 patients, the study size is considerable in this type of clinic study. Our investigation is continuing. We will update our findings as we get more detailed statistical analysis.

Method limitations and future directions. However, there is more work needed for more precise results. First, although WT at end-systole and L-curvature at end-diastole had strong correlation with the change of RVEF, the correlation is not linear and further analysis can be implemented for more precise correlation. The result of this project is an initial evaluation of the predictor. We also plan to introduce a comparison group consisted of normal persons without TOF, add this group into comparison and correlation analysis for the further conclusion. In the Methods, we introduced 4-point method to match points in longitudinal direction for L-curvature.

In this method, 4 specific points were chosen empirically. It is conceivable that different chosen points may lead to different results; we can try to choose different points and compare results to find better specific points. Or we can try to find another way to match points in longitudinal direction. Actually good match influences the results of L-curvature a lot, so searching a best way for matching points in longitudinal direction will be one key point in future work.

5. Conclusions

Pre- and post-PVR CMR data were obtained from 60 patients with repaired ToF and a CMR-based approach is introduced to obtain RV shape analysis (Curvature and Wall-thickness) to find potential predictors for post PVR surgical cardiac function outcome as measured by RV ejection fraction (RVEF). For each patient, based on the provided CMR data, we can get the contours of RV/LV. Based on these contours, we can calculate the volume of the RV before and after PVR. Then the RVEF of each patient can be calculated and used to divide the patients into two groups (one with a optimal outcome and one with suboptimal outcome). Based on the definition of curvature and wall thickness, we used a computational approach to analyze the curvature and wall thickness of each patient. We compared the results between the two outcome groups, and we also did correlation analysis between curvature/wall thickness and the change of RVEF. The comparison and correlation results indicated that WT of end systole and L-curvature of end diastole had potential to be predictors for PRV surgery outcome. The finding may shed some light for surgeons in their surgical decisions.

REFERENCES

1. Therrien J, Siu SC, McLaughlin PR. Pulmonary valve replacement in adults late after repair of tetralogy of Fallot: are we operating too late? *J Am Coll Cardiol.* 2000; 36:1670-5.
2. del Nido PJ. Surgical management of right ventricular dysfunction late after repair of Tetralogy of Fallot: right ventricular remodeling surgery, *Semin Thorac Cardiovasc SurgPediatr Card Surg Annu.* 2006; 29-34.
3. Tang D, Yang C, Geva T, del Nido PJ. Image-Based Patient-Specific Ventricle Models with Fluid-Structure Interaction for Cardiac Function Assessment and Surgical Design Optimization, *Progress in Pediatric Cardiology*, 30:51-62, 2010. PMC3041970
4. Geva T, Gauvreau K, Powell AJ, Cecchin F, Rhodes J, Geva J, del Nido P. Randomized Trial of Pulmonary Valve Replacement With and Without Right Ventricular Remodeling Surgery, *Circulation.* 2010 Sep 14;122(11 Suppl):S201-8.
5. Geva T. Introduction: magnetic resonance imaging. *Pediatr Cardiol* 21:3, 2000.
6. Keane J.F., Fyler D.C., Lock J.E. *Nadas' Pediatric Cardiology*, 2nd Edition, Saunders, 2006
7. Mulla N, Simpson P, Sullivan NM, Paridon SM. Determinants of aerobic capacity during exercise following complete repair of tetralogy of Fallot with a transannular patch. *Pediatr Cardiol.* 1997;18:350-356.
8. Nollert G, Fischlein T, Bouterwek S, Bohmer C, Dewald O, Kreuzer E, Welz A, Netz H, Klinner W, Reichart B. Long-term results of total repair of tetralogy of Fallot in adulthood: 35 years follow-up in 104 patients corrected at the age of 18 or older. *ThoracCardiovasc Surg.* 1997;45:178-181.
9. Rosenthal A. Adults with tetralogy of Fallot--repaired, yes; cured, no. *N Engl J Med,* 1993;329:655-656.

10. Vetter F. J. and McCulloch A. D., 2000, Three-dimensional stress and strain in passive rabbit left ventricle: a model study, *Annals of Biomech. Engng.* 28:781-792.
11. Geva T, Sahn DJ, Powell AJ. Magnetic resonance imaging of congenital heart disease in adults. *Progress in Pediatr Cardiol* 17: 21, 2003
12. Just H, Holubarsch C, Friedburg H. Estimation of left ventricular volume and mass by magnetic resonance imaging: comparison with quantitative biplane angiocardiography. *Cardiovasc Intervent Radiol.* 1987;10:1-4.
13. Lee D, Fuisz AR, Fan PH, Hsu TL, Liu CP, Chiang HT. Real-time 3-dimensional echocardiographic evaluation of left ventricular volume: correlation with magnetic resonance imaging--a validation study. *J Am Soc Echocardiogr.* 2001;14:1001-1009.
14. Nichols K, Saouaf R, Ababneh AA, Barst RJ, Rosenbaum MS, Groch MW, Shoyeb AH, Bergmann SR. Validation of SPECT equilibrium radionuclide angiographic right ventricular parameters by cardiac magnetic resonance imaging. *J Nucl Cardiol.* 2002;9:153-160.
15. Pini R, Giannazzo G, Di Bari M, Innocenti F, Rega L, Casolo G, Devereux RB. Transthoracic three-dimensional echocardiographic reconstruction of left and right ventricles: in vitro validation and comparison with magnetic resonance imaging. *Am Heart J.* 1997;133:221-229.
16. Powell AJ, Geva T. Blood flow measurement by magnetic resonance imaging in congenital heart disease. *Pediatr Cardiol.* 2000;21:47-58
17. Usyk TP, McCulloch AD. Relationship between regional shortening and asynchronous electrical activation in a three-dimensional model of ventricular electromechanics. *J Cardiovasc Electrophysiol.* 2003 Oct;14(10 Suppl):S196-202.

18. Brown DW, Powell AJ, Geva T. Imaging complex congenital heart disease — functional single ventricle, the Glenn circulation and the Fontan circulation: A multimodality approach. *Progress in Pediatric Cardiology* 2010;28:45–58.